

Published in final edited form as:

Mol Cancer Ther. 2024 November 04; 23(11): 1613–1625. doi:10.1158/1535-7163.MCT-23-0803.

Novel inhibition of central carbon metabolism pathways by Rac and Cdc42 inhibitor MBQ-167 and paclitaxel

Ailed M. Cruz-Collazo^{1,†}, Olga Katsara^{2,†}, Nilmary Grafals-Ruiz¹, Jessica Colon Gonzalez¹, Stephanie Dorta-Estremera^{3,4}, Victor P. Carlo⁵, Nataliya Chorna¹, Robert J Schneider^{*,2}, Suranganie Dharmawardhane^{*,1,4,6}

¹Department of Biochemistry, School of Medicine, University of Puerto Rico Medical Sciences Campus, San Juan, PR

²Department of Microbiology, New York University School of Medicine, New York, NY

³Department of Microbiology and Medical Zoology, School of Medicine, University of Puerto Rico Medical Sciences Campus, San Juan, PR

⁴Cancer Biology Division, University of Puerto Rico Comprehensive Cancer Center, San Juan, PR

⁵Department of Pathology, Auxilio Mutuo Hospital, San Juan

⁶MBQ Pharma, Inc., San Juan, PR

Abstract

Triple negative breast cancer (TNBC) represents a therapeutic challenge where standard chemotherapy is limited to paclitaxel. MBQ-167, a clinical stage small molecule inhibitor that targets Rac and Cdc42, inhibits tumor growth and metastasis in mouse models of TNBC. Herein, we investigated the efficacy of MBQ-167 in combination with paclitaxel in TNBC pre-clinical models, as a prelude to safety trials of this combination in advanced breast cancer patients. Individual MBQ-167 or combination therapy with paclitaxel was more effective at reducing TNBC cell viability and increasing apoptosis compared to paclitaxel alone. In orthotopic mouse models of human TNBC (MDA-MB-231 and MDA-MB-468), individual MBQ-167, paclitaxel, or the combination reduced mammary tumor growth with similar efficacy, with no apparent liver toxicity. However, paclitaxel single agent treatment significantly increased lung metastasis, while

Ailed M. Cruz-Collazo performed experiments, analyzed data and participated in manuscript writing. Olga Katsara performed experiments, analyzed data and participated in manuscript writing. Nilmary Grafals performed experiments and analyzed data. Stephanie Dorta-Estremera performed experiments, analyzed data and edited the manuscript. Jessica Colon González performed experiments and analyzed data, Nataliya Chorna supervised the metabolomics experiments and edited the manuscript, Victor Carlo supervised experiments and gave advise on the pathology micrographs. Robert J. Schneider designed and supervised experiments and edited the manuscript, Suranganie Dharmawardhane designed and supervised experiments and participated in manuscript writing and editing.

Authors' Disclosures

SD owns stock at MBQ Pharma, Inc., which has licensed patents US 9,981,980, US10,392,396 and international patents related to PCT/US2017/029921 relevant to this work from the University of Puerto Rico. The other authors declare no conflicts of interest.

^{*}Co-corresponding Authors: Suranganie Dharmawardhane, Department of Biochemistry, University of Puerto Rico Medical Sciences Campus, PO Box 365067, San Juan, PR 00936-5067, su.d@upr.edu; Robert Schneider, Department of Microbiology, NYU Grossman School of Medicine, New York, NY, United States. Robert.Schneider@nyumc.org.

†These authors contributed equally.

Authors' Contributions

MBQ-167, single or combined, reduced lung metastasis. In the syngeneic 4T1/BALB/c model, combined MBQ-167 and paclitaxel decreased established lung metastases by ~80%. To determine the molecular basis for the improved efficacy of the combined treatment on metastasis, 4T1 tumor extracts from BALB/c mice treated with MBQ-167, paclitaxel, or the combination were subjected to transcriptomic analysis. Gene set enrichment identified specific downregulation of central carbon metabolic pathways by the combination of MBQ-167 and Paclitaxel but not individual compounds. Biochemical validation, by immunoblotting and metabolic Seahorse analysis, shows that combined MBQ-167 and paclitaxel reduces glycolysis. This study provides a strong rationale for the clinical testing of MBQ-167 in combination with paclitaxel as a potential therapeutic for TNBC and identifies a unique mechanism of action.

Keywords

Rac; Cdc42; Rac/Cdc42 inhibitor; triple negative breast cancer; paclitaxel; combination therapy

Introduction

Triple negative breast cancer (TNBC) is an aggressive disease in which available hormone therapy is not possible and there is a lack of specific disease drivers. Consequently, optimal therapy regimens have yet to be established (1). Even though multiple targeted therapies are currently in clinical trials, anthracycline-taxane treatment is still the standard therapy for TNBC (2). However, >50% of TNBC patients become resistant to chemotherapy within 6-10 months of treatment with high risk of early relapse and death from metastasis. Moreover, TNBC that has metastasized has a poor 5-year survival rate of 12% (3). Therefore, new treatments are needed to target TNBC, particularly in the metastatic setting.

Studies on the homologous Rho GTPases Rac and Cdc42 support a pivotal role for these signaling intermediates and their downstream effector p21-activated kinase (PAK) in cancer malignancy, via regulation of migration/invasion, metastasis, epithelial to mesenchymal transition (EMT), transcription, cell proliferation, cell cycle progression, apoptosis, vesicle trafficking, angiogenesis, and cell adhesions (4,5). In addition to regulating cancer metastasis, Rac and Cdc42 are essential for Ras and other oncogenemediated transformation mechanisms (6). Rac and Cdc42 are activated by a myriad of cell surface receptors, including integrins, G-coupled protein receptors (GPCRs), growth factor receptors, and cytokine receptors that convey signals through oncogenic guanine nucleotide exchange factors (GEFs) (4,7). Moreover, numerous studies have implicated Rac/PAK activities in the maintenance of mesenchymal stem cell-like populations in epithelial cancers, as well as therapy resistance in breast cancer (8), including paclitaxel resistance in TNBC (9).

We developed MBQ-167 (9-Ethyl-3-(5-phenyl-[1,2,3]triazol-1-yl)-9H-carbazole), which inhibits Rac 1/2/3 activity with an IC $_{50}$ of 103 nM, and Cdc42 activity with an IC $_{50}$ of 78 nM (10). Similar to the previously described EHT1864 and the derivative GYS32661 (11), MBQ-167 inhibits guanine nucleotide association with Rac and Cdc42, and thus, also inhibits Rac1b, the constitutively active splice variant of Rac1, which is expressed in the

EGFR overexpressing MDA-MB-468 TNBC cell line (12). MBQ-167 inhibits viability and induces apoptosis in metastatic breast cancer cell lines and reduces stem cell like growth in mammosphere assays (10). Accordingly, MBQ-167 inhibits mammary tumor growth, metastasis and angiogenesis in mouse models of breast cancer, including TNBC (10,12,13). Therefore, MBQ-167 was granted Investigational New Drug status by the US FDA in 2022 and is currently undergoing Phase 1 clinical trials in advanced breast cancer patients (NCT06075810).

Emerging data demonstrate that chemotherapy may promote metastasis, which can be attributed to a mechanism of action that selectively kills dividing cells, thus enriching for dormant stem cell-like cancer cells with the capacity to metastasize (14). Chemotherapy may also affect the cellular interactions in the tumor microenvironment for metastasis (TMEM), and induce infiltration of perivascular macrophages, increased vascular permeability, and lymphatic penetration. Studies have also shown that paclitaxel may act directly as a ligand for Toll like receptor 4 (TLR4) expressed on macrophages and cancer cells, which is often accompanied by increased angiogenesis, cancer cell survival and invasion, and metastatic dissemination (15,16).

In the present study, we tested the hypothesis that Rac and Cdc42 inhibition by MBQ-167 can overcome paclitaxel induced cancer cell metastasis. Using pre-clinical models of human and mouse TNBC cells, we demonstrate the superior efficacy of MBQ-167 in single or combined treatments with paclitaxel. MBQ-167 is shown here to significantly reduce metastasis from the primary tumor, and importantly, to strongly reduce the burden of established lung metastases in mouse models of TNBC, in combination with paclitaxel. Genome-wide tumor transcriptomic data and biochemical validation show that MBQ-167 with paclitaxel downregulates central carbon metabolism, thus elucidating a new mechanism of action for combined MBQ-167 and paclitaxel treatment.

Materials and Methods

Cell culture

MDA-MB-231, MDA-MB-468, GFP tagged MDA-MB-231, and luciferase tagged-MDA-MB-468 and -4T1 cells were maintained in culture with Dulbecco's Modified Eagle Medium (DMEM), 10% fetal bovine serum and supplements under 5% CO2, 37°C incubation conditions. All cell lines were originally purchased from ATCC and stably transfected with green fluorescent protein (GFP) and (or) luciferase-mCherry expression using vectors containing puromycin resistance. Cells were authenticated by short tandem repeat DNA profiling by ATCC and routinely tested for the presence of *mycoplasma* by PCR assay (Sigma Aldrich).

Compounds

MBQ-167 (3-azido-9-ethyl-9*H*-carbazole 3) synthesized to 98% purity was provided by MBQ Pharma, and synthesized under GMP conditions by Galephar Pharmaceutical, Humacao, PR. MBQ-167 synthesis protocol is described in detail in (17). This protocol was adapted under GMP conditions by Galephar Pharmaceuticals, Humacao, PR, as contracted

by MBQ Pharma, Inc. For this study, MBQ Pharma supplied 98% pure MBQ-167 that was jet milled to obtain uniform particle size. This batch of MBQ-167 was characterized via differential scanning calorimetry, thermogravimetric analysis, Raman and Infrared spectroscopy, and crystal X-ray diffraction (18).

Paclitaxel (ab120143) at 98% purity was purchased from Abcam, Cambridge, UK.

Caspase assay

The Caspase-Glo 3/7 Assay from Promega was performed using the manufacturer's protocol. Cells were seeded in a 96 well plate and treated for 24, 48, 96, and 120 hours with vehicle (0.1% DMSO), MBQ-167, paclitaxel, and MBQ-167 + paclitaxel combination at the indicated concentrations. After incubation, the caspase reagent mix was added, and plates were incubated for 1h at room temperature and caspase activity quantified by luminescence.

MTT assay

The CellTiter 96 Non-Radioactive Assay (Promega) was performed using the manufacturer's protocol. Cells were seeded in a 24 well plate and treated for the indicated time with vehicle (0.1% DMSO), MBQ-167, paclitaxel or MBQ-167 + paclitaxel combination at the indicated concentrations. After incubation, the MTT (3-(4,5-dymethyl thiazol-2-yl)-2,5-diphenyl tetrazolium bromide) reagent was added, and plates were incubated for 4h at 37 °C. Stop solution was added and incubated for 1 hr at 37 °C. The absorbance of formazan was measured at 570 nm.

Animal protocol

Immunocompromised mouse studies were conducted under approved animal protocols by the University of Puerto Rico Medical Sciences Campus Institutional Animal Care and Use Committee (IACUC), in accordance with the principles and procedures outlined in the "NIH Guideline for the Care and Use of Laboratory Animals" under protocol number A8180319, as well as approval from the Office of Research Protections, Animal Care and Use Review Office of the Department of the Army, for USAMRDC proposal number BC190528, Award Number W81XWH-20-1-0041. Four to five-week-old female severe combined immunodeficiency (SCID) from Charles River Laboratories, Inc. Wilmington, MA were housed under pathogen-free conditions in HEPA-filtered cages and kept on a 12 h light/dark cycle, and controlled temperature (22-24°C), and humidity (25%). The 4T1/BALB/c models were conducted under IACUC protocol PROTO20220011 at NYU Langone. Female BALB/c mice, 6-8 weeks old were obtained from Jackson Laboratories.

Tumor establishment

GFP-tagged MDA-MB-231, or luciferase-tagged MDA-MB-468 or 4T1 cells (~2-5x10⁵), in a 1:1 suspension in buffered DMEM: Gibco Geltrex (Thermo Fisher Scientific, Waltham, MA), were injected in 100µl at the fourth right mammary fat pad of SCID mice under isofluorane inhalation. After tumor establishment (~100 mm³, ~1wk post-inoculation), animals were randomly divided into treatment groups (n=10-12).

Syngeneic mouse model

BALB/c mice were injected in the 4th mammary fat pad with 300,000 mouse 4T1 mammary carcinoma cells expressing firefly luciferase on two different occasions. To determine the effect of single or combination agent treatment (under MBQ-167 and paclitaxel treatments) on the established lung metastatic burden and to perform genome wide transcriptomic analyses. During the metastasis assay, survival surgery for primary tumor removal was performed. Tumors were excised when they reached ~150mm³ (known to have lung micromets at this tumor size in this model), the wounds were sutured, and mice were left to rest for a week. Three days upon tumor removal, lungs were visualized by bioluminescence imaging, to confirm metastatic lesions and mice were randomly distributed for treatment. For transcriptomic analyses, mice were induced with 150,000 4T1 cells and when the tumor reached ~150mm³, were randomized and treated (as mentioned below) for two weeks. At this time mice were sacrificed; tumors and lungs were collected.

MBQ-167 and paclitaxel treatments

When tumors were ~100mm³ in diameter, mice were randomized and treated with MBQ-167, paclitaxel, or MBQ-167 and paclitaxel. For experiments with immunocompromised mice, SCID mice bearing GFP-MDA-MB-231 or Luciferase-MDA-MB-468 mammary fat pad tumors (~100mm³) were treated per oral (P.O.) with vehicle (0.5% Methylcellulose and 0.1% TWEEN® 80) or MBQ-167 50.0 or 100.0 mg/kg BW (body weight) were administered via oral gavage 5X week and paclitaxel 10 mg/kg BW was administered I.P., 1X week for 3 weeks, then 1 week rest and the cycle was repeated, for a total of 136 days.

For experiments with immunocompetent mice, 150,000 syngeneic 4T1 mouse mammary carcinoma cells, expressing firefly luciferase, were injected at the 4th mammary fat pad and tumors grown to ~ 150 mm³. Primary tumors were excised and the resulting skin flap sutured on day 14. After establishment of significant metastasis to lung (Day 21) treatments were initiated as follows: (1) Control –vehicle used for MBQ167; (2) MBQ167 at 25 or 50 mg/kg in methylcellulose/Tween 80 per oral, 5 out of 7 days; (3) paclitaxel mg/kg i.p. every 5 days; (4) MBQ167 at 25 or 50 mg/kg + paclitaxel. Mice were imaged for chemiluminescence 1X a week and the study terminated on day 38 and the excised lungs imaged using a Xenogen IVIS Spectrum small animal imaging system.

For the transcriptomic analysis, BALB/c mice bearing 4T1 mouse tumors were treated on day 14 with 100 mg/kg MBQ-167 5X a week for 2 weeks and 5 mg/kg paclitaxel 1X a week. On day 28, mice were sacrificed, and the tumor extracts subjected to transcriptomic analysis.

The dosing strategy and formulation for MBQ-167 was determined from the pharmacodynamic/pharmacokinetic and toxicity studies in rodents and dogs conducted by us (13,19,20) and MBQ-Pharma, Inc., prior to Phase 1 clinical trials in humans.

Tumor growth and metastasis analysis

Initial tumor volume was measured by caliper measurements where tumor volume (mm³= $h \times l \times w \times 0.523$) were recorded once a week. When the tumors reached 100mm³, mice were randomized and grouped (N=10). Once grouped, tumor volume was determined by integrated density or total flux, respectively and monitored by fluorescence or luciferase bioluminescence imaging once a week. After completion of the study, organs were collected for metastasis analysis by fluorescence, luminescence, or H&E, and tumors were collected and analyzed. Tumor growth was determined by fluorescence or luminescence image analysis of the GFP-tagged cells in a UVP iBox Scientia dual imaging system. Relative average tumor growth was determined by the integrated density of the fluorescent tumor on each day of imaging divided by the integrated density of the same tumor on day 1 of imaging, when the treatments were started. For the assay of chemiluminescent tumors, mice were injected by I.P. with 1.5 mg luciferin, incubated for 5 min, and imaged for 5 min under white light for chemiluminescence. The size of tumors and metastatic lesions were measured by fluorescence intensity (GFP-tagged tumor cells) or total flux (chemiluminescence). In addition, the size of metastatic foci was determined by area measurements of digital images using Image J.

Flow cytometry

At the end of the experiment using luciferase-MDA-MBA-468 from scheme 2, spleens were collected, and single-cell suspensions were obtained after red blood cell lysis. The following antibodies were obtained from Biolegend (San Diego, CA) and used for flow cytometry analysis: BV421 anti-mouse CD11b (clone: 29F.1A12), PE-CF594 anti-mouse F4/80 (clone PerCPCy5.5 anti-mouse CD11c (clone: N418), PE anti-mouse CD86 (clone: GL-1), BV421 anti- mouse MHC-class II (clone: M5/114.15.2), Alexa Fluor 488 anti-mouse CD206 (clone: BV605). Live/Dead Aqua cell marker (Thermo Fisher, Waltham MA) was used to exclude dead cells. Also, anti-CD16/CD32 antibody was used to prevent non-specific binding of antibodies to Fc receptors. Stained cells were fixed with BD Cytofix/Cytoperm (BD Biosciences, San Jose CA) and prepared for acquisition on a FACSCelesta analyzer with 2 lasers (BD Biosciences, San Jose CA). Data were analyzed using FlowJo Software v10.8.1 (FlowJo, LLC, Ashland, OR).

Liver enzymes in serum

A standard comprehensive metabolic panel (ions Na, K, Cl), total protein, globulin, alkaline phosphatase, albumin, glucose, BUN creatinine, etc.) that included levels of liver enzymes aspartate aminotransferase (AST) and alanine aminotransferase (ALT) of the mice serum was performed by Core Plus clinical laboratory, Carolina, PR.

Hematoxilyn & Eosin (H&E) staining

Lungs from mice that were inoculated with luciferase-tagged MDA-MB-468 cells were extracted at necropsy and fixed in 10% formaldehyde. Fixed lungs were paraffinized and cut into 5 μ m sections. Sections were stained with a Hematoxylin & Eosin (H&E) Stain kit using a Ventana Roche automated protocol in an HE600.

Transcriptome library preparation sequencing and analysis

Three representative tumors (N=3) each were selected from mice that received vehicle and compared with mice that received 100 mg/kg MBQ-167, 5 mg/kg paclitaxel, or combined MBQ-167 (100 mg/kg) and paclitaxel (5 mg/kg). Upon excision, tumors were weighed and snap-frozen in liquid nitrogen until further processing. Equal amount of tumor tissue was homogenized using Trizol, according to the manufacturer's instructions. Total RNA was cleaned from phenol and genomic DNA contamination using the Zymo Clean and Concentrator Kit. RNA-seq libraries were prepared with 500ng of total RNA, followed by polyA selection, using the NEBNext[®] Ultra[™] II RNA Library Prep Kit for Illumina, according to the manufacturer's instructions. They were then sequenced using the Illumina NextSeq 2000 instrument in 2x55 bp paired end mode. Sequences were aligned to the GRCm38 reference genome using HISAT version 2.2.1, sorted and indexed using SAMtools (version 1.9). HTSeq (version 0.10.0) was then used to obtain the feature counts at the gene level. Differential gene expression analysis was performed using DESeq2. Each experimental group, MBQ-167, paclitaxel, or the combination was compared with vehicle controls. Gene set enrichment analysis (GSEA) was performed to identify over-represented gene sets amongst the different treatments. Overrepresentation analysis for upregulated or downregulated genes was performed using EnrichR (https://maayanlab.cloud/Enrichr/). Ingenuity Pathway Analysis (IPA, Qiagen) was performed on differentially expressed genes with a q < 0.05.

Data Availability

Raw data for this study was generated at the New York University School of Medicine Genomics core facility. The transcriptomic data has been deposited under the GEO number GSE272653 and is publicly available as of the date of publication.

Western Blotting

Tumors from the transcriptomic analysis were homogenized, and cells were lysed with lysis buffer, protein concentration was determined (DC protein, Bio Rad) and samples with equal total protein were immunoblotted for Rac1, PAK and phospho^{T423} PAK, Hexokinase I (2024S), Hexokinase II (2867S), glyceraldehyde 3-phosphate dehydrogenase (GAPDH) (2188S), total (5831S) and phospho-AMP kinase (AMPK-alpha (2535S) (Cell Signaling)and glucose-6-phosphate isomerase (GPI) (15171-1-AP, Proteintech) expression. The Oxidative Phosphorylation (Ox-Phos) rodent cocktail (ab110413, Abcam) was used to quantify relative levels of the 5 OXPHOS complexes. Actin (Sigma) and Vinculin (V4505, Sigma) were used as loading control. Image J software was used for the quantification of the integrated density of the target bands.

Seahorse Assay

The oxygen consumption rate (OCR) and extracellular acidification rate (ECAR) measurements were performed using the XF Real-Time ATP Rate Assay Kit (Agilent Technologies, Santa Clara, CA, USA) as per manufacturer's instructions. Briefly, after the determination of the optimal cell number for the assay, $2x10^4$ MDA-MB-468 cells/well were seeded in Seahorse XFe96 Analyzer (96-well plate) with 80 µL medium. The cells were

then treated with 500 nM MBQ-167, 10 nM Paclitaxel, or the combination, and incubated for 12 hours. The XFe96/XF Pro Sensor Cartridge was left overnight submerged in XF Calibrant at 37°C in a humidified non-CO₂ incubator. Cells were washed and incubated with Seahorse XF DMEM medium, pH 7.4 (supplemented with 10mM Seahorse XF Glucose, 1 mM Seahorse XF Sodium Pyruvate, 2mM Seahorse XF L-Glutamine) at 37°C without CO₂ for 60 minutes before the assay for CO₂ outgassing. The injection ports of the sensor (A, B) were loaded with 20 and 22 μ L of 15 μ M Oligomycin and 5 μ M Rotenone + Antimycin A for a final concentration of 1.5 μ M and 0.5 μ M, respectively. After calibration, three basal measurement cycles were done, followed by three measurement cycles for the injections, each consisting of a 3-minute mix and 3-minute measurements. Results were normalized for protein content. All reagents were from Agilent Technologies.

Statistical Analysis

Data statistics were done using Microsoft Excel and GraphPad Prism. Data is represented as the mean \pm SEM. To determine if there was a significant difference between the studied groups, ANOVA analysis was used and a p-value 0.05 considered significant.

Results

MBQ-167 and paclitaxel display similar toxicity profiles in vitro

We previously reported that MBQ-167 reduces the viability of MDA-MB-231 TNBC cells with a $\rm GI_{50}$ of 103 nM (10). To test the effect of combined treatment of MBQ-167 with a standard TNBC chemotherapeutic paclitaxel, we tested 250 and 500 nM of MBQ-167 and 5 ($\rm GI_{50}$ for paclitaxel) and 10 nM of paclitaxel in single and combined treatments. At 96 hrs, individual MBQ-167 at 250 or 500 nM resulted in a 60-65% decrease in cell viability, compared to vehicle treatment. Only a 25% reduction in cell viability was observed in response to 5 nM paclitaxel, while 10 nM paclitaxel resulted in a 60% decrease in cell viability compared to the vehicle. When MBQ-167 was combined with 5 or 10 nM paclitaxel, the combination resulted in a 65% reduction in cell viability, similar to individual MBQ-167 treatments (Fig. 1A).

Since we have shown that MBQ-167 induces anoikis, i.e. apoptosis due to detachment of cells from the substrate (10), caspase 3/7 activity was monitored to determine the effect of individual or combined MBQ-167 and paclitaxel on apoptosis. MBQ-167 at 250 nM increased apoptosis significantly by 1.8-fold, while prolonged 500 nM treatment resulted in a loss of polarity, detachment from the substrate, and cell shrinkage indicative of cell death, as previously reported (10). Therefore, the increase in caspase 3/7 activity was not as evident at 500 nM because the cells had completed apoptosis, and all organelles and molecules were fragmented. As expected, paclitaxel at 5 and 10 nM exerted the highest effect on apoptosis, which were also evident in combination with MBQ-167 (Fig. 1B). These data demonstrate that MBQ-167 is effective in decreasing cell viability with equal efficacy as paclitaxel but does not exert additive or synergistic effects with paclitaxel on cell viability.

MBQ-167 strongly reduces tumor growth in TNBC mouse models in single or combined treatments with paclitaxel

We first determined the correct regimen for paclitaxel treatment by administering MBQ-167 and paclitaxel in various concentrations to BALB/c immunocompetent mice. None of the MBQ-167 treatments resulted in morphological or liver enzyme changes. However, 2X a week treatment with 5 or 10 mg/kg BW paclitaxel resulted in severe constipation, reduced survival and increases in alanine transaminase activity from plasma (21). Therefore, the regimen of paclitaxel treatment was reduced to 5 or 10 mg/kg BW 1X a week for 3 weeks, followed by a rest for 1 week and resumed on week 5 for a further 3 weeks.

Next, we tested the effect of MBQ-167 and paclitaxel single or combination treatments in immunocompromised SCID mice bearing ~100 mm³ GFP-MDA-MB-231 TNBC tumors. Mice were treated with vehicle, 50 or 100 mg/kg MBQ-167 (P.O., 5X week), paclitaxel 10 mg/kg (I.P. 1X week for 3 weeks and 1 week rest cycle), or a combination of MBQ-167 (50 or 100mg/kg) and paclitaxel (10mg/kg). Tumor growth was quantified weekly by fluorescence image analysis and mice were sacrificed at 70 days. MBQ-167 reduced tumor growth by ~70% compared to vehicle. Single or combined treatment with paclitaxel also reduced tumor growth to a similar extent (Fig. 1 C,D). Mouse body weight was also analyzed for the effect of the treatments and did not show any change. Moreover, this combination of treatments did not affect liver enzyme activities from plasma (Fig. 1E). Therefore, the administered paclitaxel treatment cycle or the combinations were not toxic to the mice. Since most of the vehicle mice did not show sufficient metastases in this study, we were not able to analyze the effect on metastases in a statistically significant manner.

MBQ-167 reduces lung metastasis in TNBC mouse models in single or combined treatments with paclitaxel

We tested the effect of single and (or) combined treatments of MBQ-167 with paclitaxel in an aggressive epidermal growth factor receptor (EGFR) overexpressing MDA-MB-468 cell line, which also expresses wildtype Rac1/3 and the oncogenic Rac1B splice variant. We recently demonstrated that MBQ-167 is effective at inhibiting wildtype Rac and Cdc42 as well as Rac1B in MDA-MB-468 cells (12). Tumor growth was assessed 1X a week by chemiluminescence imaging. Oral gavage of 50 or 100 mg/kg BW MBQ-167, administered for 136 days, resulted in a ~90% statistically significant decrease in tumor growth, similar to paclitaxel alone, or the combination (Fig. 2 A,B). Single or combined treatments did not result in any significant changes in weight or physical appearance compared to vehicle treatments (Fig. 2C).

When the mice were assessed for lung metastases at necropsy, by chemiluminescence of extracted lungs, 50 mg/kg BW MBQ-167 treatment abolished all lung metastases. Paclitaxel treatment induced 1.7-fold increase in lung metastases, which was reduced by MBQ-167 treatment in combination (Fig. 3A). This effect was confirmed by H&E staining of fixed lungs, where vehicle treatment and paclitaxel single treatment resulted in 2-3 large metastatic foci/microscopic field/section at 10X (Fig. 3B). Single or combined MBQ-167 treatment significantly reduced lung metastatic foci number (Fig. 3C), as well as size of individual foci (Fig. 3D) by ~70%.

Since the small GTPases Rac and Cdc42 serve as critical molecular targets that regulate both cancer cell and immune cell function at the tumor microenvironment (22), we tested the contribution of MBQ-167 and paclitaxel to macrophage counts during treatment. Therefore, at necropsy, spleens were harvested and subjected to flow cytometry to determine the effect of MBQ-167, paclitaxel, or MBQ-167 and paclitaxel on CD11b, F4/80⁺ myeloid cells. M1 vs M2 immunosuppressive macrophages were distinguished by using the CD206 marker, which is expressed on CD11b+F4/80+ M2 macrophages. Paclitaxel treatment to mice bearing MDA-MB-468 mammary fatpad tumors, resulted in an increase in the percentage of M1 and M2 macrophages, which was reduced by MBQ-167 treatment either individually or in combination, which was more evident in the M2 macrophage counts (Suppl. Fig. 1). Therefore, MBQ-167 may exert additional anti-cancer effects through suppression of increased M2 macrophages following paclitaxel treatment.

MBQ-167 reduces the viability of established lung metastases in single or combination therapy with paclitaxel

Since our experiments with human TNBC spontaneous metastasis mouse models demonstrated that MBQ-167 in combination with paclitaxel reduced metastasis, we evaluated the capacity of MBQ-167 to target established metastases in a syngeneic mouse TNBC model (Supp. Table 1). As shown in Fig. 4A, BALB/c mice were injected with syngeneic 4T1 mammary carcinoma cells expressing firefly luciferase, tumors grown to ~ 250-300 mm³, and tumors excised (Fig. 4B,C). After establishment of significant metastasis to lung, treatments were initiated as follows: (1) Control –vehicle used for MBQ167; (2) MBQ167 at 25 or 50 mg/kg in methylcellulose/Tween 80 by oral gavage, 5 out of 7 days; (3) paclitaxel (PTX) 5 mg/kg i.p. every 5 days; (4) MBQ-167 at 25 or 50 mg/kg + PTX. Data show a >99% reduction in established lung metastasis with combination treatment of 50 mg/kg MBQ167 with PTX compared to untreated control. This is even more remarkable considering that PTX alone resulted in a several-fold increase in lung metastatic burden compared to untreated controls. MBQ-167 single agent did not reduce metastatic tumor burden at either concentration. In conclusion, MBQ-167 at 50 mg/kg was well tolerated, and when combined with paclitaxel, shows an almost complete shrinkage of established lung metastases in a syngeneic and highly aggressive mouse model of breast cancer (Fig. 4D-F).

MBQ-167 downregulates expression of inflammatory pathway genes and upregulates death receptor signaling

To determine the molecular basis of the beneficial effects of MBQ-167, paclitaxel, or the combination, BALB/c mice with 4T1 mammary fat pad tumors (~100 mm³) were treated with 100 mg/kg BW MBQ-167 5X a week by oral gavage for 2 weeks or paclitaxel at 5 mg/kg BW 1X a week for 2 weeks or the combination (Suppl. Fig. 2A). At the end of 2 weeks, mice were necropsied, and the extracted tumors processed for transcriptomic analysis. When compared with vehicle controls, genome-wide transcriptomic analysis (n=3) discovered 905, 315 and 387 differentially expressed genes in paclitaxel, 100 mg/kg BW MBQ-167, and combination therapy respectively, with a q value <0.05 (Suppl Fig. 2B-G).

As per Ingenuity Pathway Analysis (IPA), several metastasis and immune regulatory pathways were significantly downregulated in response to MBQ-167 treatment (Suppl.

Fig., 2 H,I,J; Suppl. Table 2). Notably, the S100 family signaling pathway, including S100A6, S100A8, S100A9, and S100A10, which regulates metastasis and inflammatory signaling (23,24), were all significantly downregulated. As expected, Rho family signaling, Hypoxia Inducible Factor (HIF)-1a signaling and Interleukin-6 (IL-6) signaling were also downregulated. Upregulated pathways in response to individual MBO-167 included death receptor signaling, macrophage activation, IL-7 and IL-10 signaling, and necroptosis signaling (Suppl. Fig. 2H). Therefore, MBQ-167 may exert immunoprotective effects by downregulating IL-6 signaling, as was recently reported by us (25), and upregulating IL-7 signaling which has been implicated in anti-tumor immunity (26). Interestingly, paclitaxel alone downregulated HIf-1a signaling, glycolysis, actin cytoskeleton, RhoA and CXCR4 signaling, while upregulating several cell death mechanisms, such as death receptor signaling, necroptosis, and pyroptosis (Suppl. Fig. 2I). The combination treatment differentially regulated some genes that were also regulated by individual MBQ-167 or paclitaxel, or the combination, such as downregulation of glycolysis, CXCR4 signaling, IL-6 signaling, and upregulation of death receptor and IL-10 signaling. Paclitaxel downregulated glycolysis genes ALDOA, ENO1, GPI, PFKL, PKM, and TPL1 by a Z score of -2.4, with a more marked decrease in the combined treatment (Suppl.Fig. 2J, Suppl. Table 2).

Combined therapy of MBQ-167 with paclitaxel downregulates central carbon metabolism

GSEA comparing combination treatment to vehicle treated controls, identified four significant downregulated pathways, all involved in carbon metabolism, with a positive normalized enrichment score (NES) and an FDR q-value <0.1 (Fig. 5A). A representative heat map of the top 20 downregulated genes of the most affected pathway, central carbon metabolism in cancer, is shown (Fig. 5B), and representative enrichment plots were developed for all four pathways (Fig. 5C). Of particular interest are mRNAs of proteins that are major players in glycolysis, such as hexokinase-1 (HK1), glucose-6phosphate dehydrogenase-X (G6PDX), and pyruvate kinase (PKM). In addition, analyzing the significantly downregulated genes using EnrichR, a method that identifies biological functions that are overrepresented in the dataset, found that the combination treatment regimen of MBQ-167 plus paclitaxel not only inhibited expression of genes regulating major metabolic pathways, but also downregulated genes important for tumor angiogenesis, cytoskeletal regulation and integrin signaling pathways, all major pathways involved in the metastatic process of TNBC (Fig. 5D,E). Furthermore, gene ontology (GO) biological process analysis discovered an effect on neutrophils that have been recently shown to play a major role in the generation of the pre-metastatic niche and, thus, contribute to the metastatic process of TNBC (Fig. 5F) (27).

Figure 6 and Supplemental Table 2 demonstrate that key genes that play a major role in the glycolysis pathway were differentially expressed from tumors of mice that received the MBQ-167 and paclitaxel combination, compared to vehicle or individual treatments. Therefore, those proteins whose function has been implicated in cell survival, apoptosis and metastases in TNBC but also were at least two-fold downregulated on the mRNA level, were selected for validation via Western blot from the same tumors used for the transcriptomic analysis. The top downregulated genes in response to the combination treatment, Hexokinase I and II, were also significantly downregulated in protein expression,

as well as GAPDH and GPI1 proteins (Fig. 6A, B). Another gene set that was significantly downregulated and identified from the ingenuity pathway analysis (IPA) analysis for top Glycolysis pathway genes was that of Aldolase A and C (Suppl. Table 2). Downregulation of Aldolase is known to downregulate the expression of AMP kinase α (AMPKα) and increase its function of acting as a switch between glycolysis and oxidative phosphorylation (28). Therefore, the levels and activity of AMPKα were quantified from Western blots and demonstrate a reduction of AMPKα expression in tumors of mice that received the combination treatment; however, there was a ~two-fold increase in AMPKα activity, as measured by T172 phosphorylation (Fig. 6C-E). That led us to further investigate using Seahorse analysis but also by Western blot analysis of key proteins of the five Ox-Phos complexes. An increase in the expression of complex III and IV as indicated by increased ubiquinol cytochrome C reductase core protein 2 (uqcrc2) and mitochondrial encoded cytochrome oxidase (Mtco1) expression was observed without significant changes in protein expression of the other complexes (Figure 6 F,G).

Seahorse analysis of Oxygen consumption rate (OCR) and extracellular acidification rate (ECAR) in MDA-MB-468 triple negative breast cancer cells show that OCR is not affected by individual or combined MBQ-167 and paclitaxel. However, ECAR, which measures acidification due to lactate produced during glycolysis is significantly decreased in the combined treatment in comparison to vehicle treatment, as well as individual MBQ-167 or paclitaxel (Fig. 6H). Moreover, the glycolytic ATP production rate, but not the mitochondrial ATP production rate, is reduced by combined MBQ-167 and paclitaxel (Suppl. Fig. 3). Taken together these results show that the combination treatment of MBQ-167 and paclitaxel downregulates key glycolytic pathway proteins to result in reduced glycolysis.

Discussion

TNBC constitutes a heterogeneous group of malignancies that are typically aggressive and associated with a poor prognosis. Lack of targeted therapies and the inherent heterogeneity of TNBC makes uniform treatment challenging, and optimal therapy regimens have yet to be established (1). Even though multiple targeted therapies including immune checkpoint therapies are currently in clinical trials (29), paclitaxel is still the standard therapy for TNBC (30).

Herein, we tested the efficacy of MBQ-167, a potent Rac and Cdc42 inhibitor developed by us, which we have shown to inhibit tumor growth and metastasis, as well as overcome EGFR therapy resistance in several pre-clinical breast cancer models (10,12,13,31). We show that MBQ-167 is equal to paclitaxel in reducing cell growth and inducing apoptosis. Previously, we have shown that MBQ-167 reduces cell viability through anoikis, i.e. apoptosis due to loss of cell to substrate attachments (17). Since the combination of MBQ-167 and paclitaxel was not significantly different from single treatments of either compound, we conclude that the combination treatment has no additive or synergistic effects on cell survival of TNBC cells. These results are validated by the mouse studies where MDA-MB-231, MDA-MB-468, or 4T1 mammary fat pad tumors in immune-compromised and -competent mice treated with MBQ-167 or paclitaxel (single or combined), significantly reduced tumor growth with equal efficacy (Suppl. Table 1). This is corroborated by the transcriptomic

analysis of tumors from mice where individual MBQ-167 or paclitaxel treatment activated similar signaling pathways such as death receptor signaling, and downregulated Rho GTPase signaling. However, each individual compound (MBQ-167 or paclitaxel) also acts independently through multiple pathways to reduce tumor growth. Therefore, the observed reduction in tumor growth is expected to be due to similar and distinct pathways that do not synergize but reduce tumor growth to the same extent.

The salient observation that MBQ-167 reduced the paclitaxel-induced metastases in aggressive pre-clinical models is highly relevant for its translational development as a viable TNBC therapeutic. Especially, in the more aggressive MDA-MB-468 cell line, which overexpresses EGFR, a potent activator of Rac (32), MBQ-167 inhibits activation of both Rac and the Rac1B constitutively active splice form (12). Accordingly, we found MBQ-167 to be highly effective at reducing both primary tumors and metastases from MDA-MB-468 mammary tumors (Figs. 2,3, Suppl. Table 1).

Even more striking is that the combination of MBQ-167 and paclitaxel strongly reduces established lung metastases from the 4T1 aggressive mouse TNBC cell line. We recapitulated a typical clinical scenario in this study by excising the primary tumors following establishment of lung metastases prior to treatment. While MBQ-167 alone was not sufficient to eliminate all lung metastases, combination treatment with paclitaxel was highly effective, whereas paclitaxel alone demonstrated metastatic progression in treated mice. However, MBQ-167 significantly reduced lung metastases in number and size of metastatic foci; thereby demonstrating its strong potential in combination therapy with paclitaxel (Fig. 4).

It is well established that chemotherapy can result in the preferential killing of dividing cells, thus selecting for dormant cells with the potential for metastatic colonization (33,34). In fact, several reports have shown that even though paclitaxel reduces primary tumor growth due to its inhibitory effect on dividing cells, it has the potential to increase metastasis, particularly through activation of TLR4 (15). We have shown that MBQ-167 can specifically reduce mammosphere formation, which is indicative of stem cell-like activity (10), which may account for the observed inhibition of metastasis in response to paclitaxel by MBQ-167. In addition to reducing dormant cell activity, Rac and Cdc42 inhibition may directly suppress paclitaxel induced TLR4 activation of NF-κB activity, leading to increased inflammation and metastasis (35).

The effect of MBQ-167 on both pro-tumor inflammation and metastasis is further validated by the transcriptomic analysis (Fig. 5, Suppl. Fig. 2, Suppl. Table 2), where we found downregulation of genes regulating cancer progression from tumors of mice receiving MBQ-167. MBQ-167, as well as the combination treatment, downregulated Rho family signaling and HIF-1a signaling, which are expected to reduce metastasis via inhibition of actin cytoskeletal regulation as well as malignant signaling induced by hypoxia (4,36). HIF1a is critical for cancer stem cell survival, angiogenesis and metastasis, and is known to be regulated by Rac1 signaling (37,38). In addition, CXCR4 signaling, a central mediator of VEGF-mediated angiogenesis (39), is also significantly downregulated by the combination treatment. Other notable pathways unique to MBQ-167 downregulation,

include inflammatory markers secreted by cancer cells, as well as macrophages and neutrophils, such as S100A protein signaling which regulates inflammatory mechanisms in cancer, as well as interleukin-6 (IL-6), a cytokine that promotes inflammation in cancer (23,40-43). Accordingly, we recently demonstrated that IL-6 secretion is reduced by Rac/Cdc42 inhibitors in breast cancer models (22). We also recently reported reduced tumor macrophages, myeloid derived suppressor cells, but not monocytes in breast tumors as well as spleens using human breast cancer cells in SCID mice as well as in the 4T1/BALB/c model in response to MBQ-167 (22). Therefore, the effects of MBQ-167 may also contribute to the observed decrease in macrophages in spleens from mice treated with MBQ-167 or the combination, but not individual paclitaxel treatment. Intriguingly, the transcriptomic analysis also highlighted that the combination of MBQ-167 and paclitaxel modulated the function of neutrophils potentially through the induction of degranulation and/or release of neutrophil extracellular traps. Therefore, the combination of MBQ-167 and paclitaxel may have additional immunomodulatory effects on the tumor microenvironment from TNBC.

Strikingly, transcriptomic analysis of tumors from mice that received MBQ-167 and paclitaxel identified downregulation of central carbon metabolism may contribute to the efficacy of combined therapy. Even though paclitaxel alone reduced some glycolysis pathway genes, the GSEA analysis demonstrated that the combination alone significantly reduced carbon metabolism, including fructose and mannose metabolism and specifically glycolysis. Notably, our data show that several genes encoding key glycolytic enzymes, such as HK1 and HK2, pyruvate kinase (PKM), several phosphofructokinases (PFK), Lactose dehydrogenase (LDHA), which has been implicated in Rac1 activation in breast cancer (44), G6PDX, phosphoglycerate mutase (PGAM1), and Phosphatidyl inositol 3-kinase (PIK3R2), are significantly downregulated in tumors with the combination treatment; thus signifying a dramatic inhibitory effect on glycolysis. The effect on downregulation of carbon metabolism was confirmed by demonstrating that both gene and protein expression of HK1 and HK2, key enzymes that convert glucose to glucose 6-phosphate, were significantly downregulated from tumors of mice that received the combination treatment compared to tumors from vehicle treated mice. Alterations in metabolic enzymes, particularly glycolytic enzymes that promote the Warburg effect, play a central role in cancer progression, metastasis, and therapy resistance (45).

Western blot analysis of tumor extracts also supports a role for glycolysis being the major pathway downregulated by the combination treatment, where key mitochondrial complex proteins that participate in oxidative phosphorylation were not significantly affected by the combination treatment. This is also validated by the Seahorse analysis of breast cancer cells following vehicle or combined MBQ-167 and paclitaxel, where OCRs remained unchanged, while ECAR, which measures the lactate released in the glycolytic pathway, was decreased in the combination treatment, compared to vehicle or individual MBQ-167 or paclitaxel treatments (Fig. 6, Suppl. Fig. 3). This may be attributed to a combined effect of the stress caused by the combination treatment (via both MBQ-167 and paclitaxel) inducing apoptotic pathways, which can adversely affect metabolism. Moreover, emerging data has implicated Rac and Cdc42 in glucose metabolism, and thus, cancer progression (46). Rac1 has been implicated in glucose metabolism in colon cancer (47), and Rac inhibition has been shown to overcome therapy resistance in hepatocellular and esophageal squamous

carcinoma through downregulation of glycolytic enzymes (48,49). Therefore, MBQ-167 may also contribute to the observed inhibitory effects on glycolysis via Rac inhibition.

The observed downregulation of metabolism in response to combined MBQ-167 and paclitaxel may, at least be partially, attributed to reduced AKT/mTOR signaling. AKT/mTOR has been implicated in regulation of glycolysis via Rac signaling (50). Our results show that mRNA levels of *Akt* were significantly downregulated in the combination treatment, which also include glucose transporters SLC2A1 and SLC16A3, which are increased by AKT activation. In addition, the significant downregulation of mitogen activated protein kinases (MAP2K1, MAP2K2, MAPK3) would also contribute to the synergistic inhibition of metastasis by the combination treatment.

Given the highly reduced number and size of lung metastases, we did not obtain sufficient metastatic tissue from mice that received MBQ-167 or the combination. Therefore, we had to use primary tumors to elucidate the mechanism underlying the inhibition of metastasis, a stochastic process, which includes invasion, intravasation, survival in the circulation, extravasation, and establishment and growth of lung metastases. The results presented herein, only show the significant transcriptomic and proteomic changes in the tumors from mice that received the combination treatment. Since the rate of tumor growth inhibition was similar for individual treatments, while individual paclitaxel treatment increased metastasis, and MBQ-167 or the combination reduced metastasis to the lung, the inhibitory effect on carbon metabolism by the combination treatment parallels the drastic reduction in metastasis. The observed downregulation of glycolysis in tumor cells following combination therapy with MBQ-167 and paclitaxel may correlate with decreased cellular energy production, and consequently, their ability to establish distant metastases. Since most cancer cells rely on glycolysis to generate ATP even when oxygen is available, glycolysis directly contributes to tumor metastasis, which is an energy intensive process (51,52). Therefore, the inhibition of glycolysis by combined MBQ-167 and paclitaxel is thought to contribute to the inhibition of metastasis in response to the combined treatment, but not paclitaxel.

In cancer patients, paclitaxel is usually given 1X week, with ~3 weeks of rest between cycles (53). Our studies also demonstrated that paclitaxel needs to be carefully administered at low concentrations at infrequent time intervals, whereas MBQ-167 can be administered 5X a week with a NOAEL of 1000 mg/kg BW in pre-clinical models. Therefore, MBQ-167 has the potential to be less toxic and as effective as paclitaxel in reducing tumor growth and thus, may be effective as an alternative therapeutic strategy for TNBC.

In conclusion, this study validates MBQ-167 as a TNBC therapeutic with a similar effect as paclitaxel in reducing tumor growth, with the additional benefit of also inhibiting metastasis. Moreover, MBQ-167 is a viable candidate for combination treatment with paclitaxel in TNBC to target metastasis and acquired resistance. Once, the Phase 1 trial for MBQ-167 is completed (NCT06075810), future clinical trials of MBQ-167 in combination with paclitaxel is expected to demonstrate its utility in TNBC metastasis prevention and cure.

Supplementary Material

Refer to Web version on PubMed Central for supplementary material.

Financial support:

Financial support was provided by NIH/NIGMS SC3GM084824, and US Army Breast Cancer Research Program (BCRP) W81XWH2010041 and HT9425-23-1-0166 grants (to SD), NIH/NIGMS 5P20GM103475 (to ACC and NC), NIGMS-RISE R25GM061838 (to JCG), and BCRF-22-146, NIH/NCI R01CA248397, US Army/BCRP HT9425-23-1-0166 and funds from MBQ Pharma, Inc. (to RJS).

References

- Lehmann BD, Pietenpol JA, Tan AR. Triple-negative breast cancer: molecular subtypes and new targets for therapy. Am Soc Clin Oncol Educ book Am Soc Clin Oncol Annu Meet. Am Soc Clin Oncol Educ Book; 2015;e31–9.
- 2. Furlanetto J, Loibl S. Optimal Systemic Treatment for Early Triple-Negative Breast Cancer. Breast Care (Basel). Breast Care (Basel); 2020;15:217–26. [PubMed: 32774215]
- Baranova A, Krasnoselskyi M, Starikov V, Kartashov S, Zhulkevych I, Vlasenko V, et al. Triplenegative breast cancer: current treatment strategies and factors of negative prognosis. J Med Life. J Med Life; 2022;15:153–61. [PubMed: 35419095]
- 4. Del Mar Maldonado M, Dharmawardhane S. Targeting rac and Cdc42 GT pases in cancer. Cancer Res. American Association for Cancer Research Inc.; 2018. page 3101–11.
- 5. Heasman SJ, Ridley AJ. Mammalian Rho GTPases: new insights into their functions from in vivo studies. Nat Rev Mol Cell Biol. Nat Rev Mol Cell Biol; 2008;9:690–701. [PubMed: 18719708]
- 6. Qiu RG, Chen J, Kirn D, Mc Cormick F, Symons M. An essential role for Rac in Ras transformation. Nature. Nature; 1995;374:457–9. [PubMed: 7700355]
- 7. Maldonado MDM, Medina JI, Velazquez L, Dharmawardhane S. Targeting Rac and Cdc42 GEFs in Metastatic Cancer. Front cell Dev Biol. Frontiers Media S.A.; 2020;8:201. [PubMed: 32322580]
- Cardama GA, Alonso DF, Gonzalez N, Maggio J, Gomez DE, Rolfo C, et al. Relevance of small GTPase Rac1 pathway in drug and radio-resistance mechanisms: Opportunities in cancer therapeutics. Crit Rev Oncol Hematol. Crit Rev Oncol Hematol; 2018;124:29–36. [PubMed: 29548483]
- 9. Oudin MJ, Barbier L, Schäafer C, Kosciuk T, Miller MA, Han S, et al. MENA Confers Resistance to Paclitaxel in Triple-Negative Breast Cancer. Mol Cancer Ther. Mol Cancer Ther; 2017;16:143–55. [PubMed: 27811011]
- Humphries-Bickley T, Castillo-Pichardo L, Hernandez-O'Farrill E, Borrero-Garcia LD, Forestier-Roman I, Gerena Y, et al. Characterization of a dual Rac/Cdc42 Inhibitor MBQ-167 in metastatic cancer. Mol Cancer Ther; 2017;16:805–18. [PubMed: 28450422]
- 11. Bailly C, Beignet J, Loirand G, Sauzeau V. Rac1 as a therapeutic anticancer target: Promises and limitations. Biochem Pharmacol. Biochem Pharmacol; 2022;203.
- Medina JI, Cruz-Collazo A, Maldonado M del M, Matos Gascot T, Borrero-Garcia LD, Cooke M, et al. Characterization of Novel Derivatives of MBQ-167, an inhibitor of the GTP-binding proteins Rac/Cdc42. Cancer Res Commun. Cancer Res Commun; 2022;2:1711–26. [PubMed: 36861094]
- Cruz-Collazo A, Ruiz-Calderon JF, Picon H, Borrero-Garcia LD, Lopez I, Castillo-Pichardo L, et al. Efficacy of Rac and Cdc42 Inhibitor MBQ-167 in Triple-negative Breast Cancer. Mol Cancer Ther. Mol Cancer Ther; 2021;20:2420–32. [PubMed: 34607932]
- 14. Karagiannis GS, Condeelis JS, Oktay MH. Chemotherapy-Induced Metastasis: Molecular Mechanisms, Clinical Manifestations, Therapeutic Interventions. Cancer Res. Cancer Res; 2019;79:4567–77. [PubMed: 31431464]
- 15. Volk-Draper L, Hall K, Griggs C, Rajput S, Kohio P, DeNardo D, et al. Paclitaxel therapy promotes breast cancer metastasis in a TLR4-dependent manner. Cancer Res. Cancer Res; 2014;74:5421–34. [PubMed: 25274031]

16. Byrd-Leifer CA, Block EF, Takeda K, Akira S, Ding A. The role of MyD88 and TLR4 in the LPS-mimetic activity of Taxol. Eur J Immunol. Germany; 2001;31:2448–57. [PubMed: 11500829]

- 17. Humphries-Bickley T, Castillo-Pichardo L, Hernandez-O'Farrill E, Borrero-Garcia LD, Forestier-Roman I, Gerena Y, et al. Characterization of a Dual Rac/Cdc42 Inhibitor MBQ-167 in Metastatic Cancer. Mol Cancer Ther. 2017;16:805–18. [PubMed: 28450422]
- 18. Jiménez Cruz JM, Vlaar CP, Stelzer T, López-Mejías V. Polymorphism in early development: The account of MBQ-167. Int J Pharm. NIH Public Access; 2021;608:121064. [PubMed: 34481010]
- Reig-López J, Maldonado MDM, Merino-Sanjuan M, Cruz-Collazo AM, Ruiz-Calderón JF, Mangas-Sanjuán V, et al. Physiologically-Based Pharmacokinetic/Pharmacodynamic Model of MBQ-167 to Predict Tumor Growth Inhibition in Mice. Pharmaceutics. MDPI AG; 2020;12:1–17.
- 20. Del Mar Maldonado M, Rosado-González G, Bloom J, Duconge J, Ruiz-Calderón JF, Hernández-O'Farrill E, et al. Pharmacokinetics of the Rac/Cdc42 Inhibitor MBQ-167 in Mice by Supercritical Fluid Chromatography-Tandem Mass Spectrometry. ACS Omega. American Chemical Society; 2019;4:17981–9. [PubMed: 31720502]
- Cruz-Collazo AM. Novel Approaches to Targeting Breast Cancer Metastasis. University of Puerto Rico Medical Sciences Campus; 2021.
- 22. Torres-Sanchez A, Rivera-Robles M, Castillo-Pichardo L, Martínez-Ferrer M, Dorta-Estremera SM, Dharmawardhane S. Rac and Cdc42 inhibitors reduce macrophage function in breast cancer preclinical models. Front Oncol. Front Oncol; 2023;13.
- 23. Markowitz J, Carson WE. Review of S100A9 biology and its role in cancer. Biochim Biophys Acta. Biochim Biophys Acta; 2013;1835:100–9. [PubMed: 23123827]
- 24. Simeonov KP, Byrns CN, Clark ML, Norgard RJ, Martin B, Stanger BZ, et al. Single-cell lineage tracing of metastatic cancer reveals selection of hybrid EMT states. Cancer Cell. Cancer Cell; 2021;39:1150–1162.e9. [PubMed: 34115987]
- Saraiva M, Vieira P, O'Garra A. Biology and therapeutic potential of interleukin-10. J Exp Med. J Exp Med; 2020;217.
- 26. Lin J, Zhu Z, Xiao H, Wakefield MR, Ding VA, Bai Q, et al. The role of IL-7 in Immunity and Cancer. Anticancer Res. Anticancer Res; 2017;37:963–7. [PubMed: 28314253]
- 27. Zheng C, Xu X, Wu M, Xue L, Zhu J, Xia H, et al. Neutrophils in triple-negative breast cancer: an underestimated player with increasingly recognized importance. Breast Cancer Res. Breast Cancer Res; 2023;25.
- 28. Zhang CS, Hawley SA, Zong Y, Li M, Wang Z, Gray A, et al. Fructose-1,6-bisphosphate and aldolase mediate glucose sensing by AMPK. Nature. Nature; 2017;548:112–6. [PubMed: 28723898]
- 29. Schettini F, Venturini S, Giuliano M, Lambertini M, Pinato DJ, Onesti CE, et al. Multiple Bayesian network meta-analyses to establish therapeutic algorithms for metastatic triple negative breast cancer. Cancer Treat Rev. Cancer Treat Rev; 2022;111.
- 30. Lebert JM, Lester R, Powell E, Seal M, McCarthy J. Advances in the systemic treatment of triple-negative breast cancer. Curr Oncol. Curr Oncol; 2018;25:S142–50. [PubMed: 29910657]
- 31. Borrero-García LD, del Mar Maldonado M, Medina-Velázquez J, Troche-Torres AL, Velazquez L, Grafals-Ruiz N, et al. Rac inhibition as a novel therapeutic strategy for EGFR/HER2 targeted therapy resistant breast cancer. BMC Cancer. BMC Cancer; 2021;21.
- 32. Cooke M, Kreider-Letterman G, Baker MJ, Zhang S, Sullivan NT, Eruslanov E, et al. FARP1, ARHGEF39, and TIAM2 are essential receptor tyrosine kinase effectors for Rac1-dependent cell motility in human lung adenocarcinoma. Cell Rep. Cell Rep; 2021;37.
- 33. Massagué J, Ganesh K. Metastasis-Initiating Cells and Ecosystems. Cancer Discov. 2021;11:971–94. [PubMed: 33811127]
- 34. Middleton JD, Stover DG, Hai T. Chemotherapy-Exacerbated Breast Cancer Metastasis: A Paradox Explainable by Dysregulated Adaptive-Response. Int J Mol Sci. Int J Mol Sci; 2018;19.
- 35. Gastonguay A, Berg T, Hauser AD, Schuld N, Lorimer E, Williams CL. The role of Rac1 in the regulation of NF-κB activity, cell proliferation, and cell migration in non-small cell lung carcinoma. Cancer Biol Ther. Cancer Biol Ther; 2012;13:647–56. [PubMed: 22549160]
- 36. Pezzuto A, Carico E. Role of HIF-1 in Cancer Progression: Novel Insights. A Review. Curr Mol Med. Curr Mol Med; 2018;18:343–51. [PubMed: 30411685]

37. Abd GM, Laird MC, Ku JC, Li Y. Hypoxia-induced cancer cell reprogramming: a review on how cancer stem cells arise. Front Oncol. Front Oncol; 2023;13.

- 38. Hirota K, Semenza GL. Rac1 activity is required for the activation of hypoxia-inducible factor 1. J Biol Chem. J Biol Chem; 2001;276:21166–72. [PubMed: 11283021]
- 39. Liang Z, Brooks J, Willard M, Liang K, Yoon Y, Kang S, et al. CXCR4/CXCL12 axis promotes VEGF-mediated tumor angiogenesis through Akt signaling pathway. Biochem Biophys Res Commun. Biochem Biophys Res Commun; 2007;359:716–22. [PubMed: 17559806]
- 40. Libreros S, Garcia-Areas R, Shibata Y, Carrio R, Torroella-Kouri M, Iragavarapu-Charyulu V. Induction of proinflammatory mediators by CHI3L1 is reduced by chitin treatment: decreased tumor metastasis in a breast cancer model. Int J cancer. Int J Cancer; 2012;131:377–86. [PubMed: 21866546]
- 41. Kumari N, Dwarakanath BS, Das A, Bhatt AN. Role of interleukin-6 in cancer progression and therapeutic resistance. Tumour Biol. Tumour Biol; 2016;37:11553–72. [PubMed: 27260630]
- 42. Qi Y, Zhang Y, Li J, Cai M, Zhang B, Yu Z, et al. S100A family is a group of immune markers associated with poor prognosis and immune cell infiltration in hepatocellular carcinoma. BMC Cancer. BMC Cancer; 2023;23.
- 43. Rašková M, Lacina L, Kejík Z, Venhauerová A, Skali ková M, Kolá M, et al. The Role of IL-6 in Cancer Cell Invasiveness and Metastasis-Overview and Therapeutic Opportunities. Cells. Cells; 2022;11.
- 44. Osaka N, Sasaki AT. Beyond Warburg: LDHA activates RAC for tumour growth. Nat Metab. Nat Metab; 2022;4:1623–5. [PubMed: 36536138]
- 45. Jaworska M, Szczudło J, Pietrzyk A, Shah J, Trojan SE, Ostrowska B, et al. The Warburg effect: a score for many instruments in the concert of cancer and cancer niche cells. Pharmacol Rep. Pharmacol Rep; 2023;75:876–90. [PubMed: 37332080]
- 46. Møller LLV, Klip A, Sylow L. Rho GTPases-Emerging Regulators of Glucose Homeostasis and Metabolic Health. Cells. Cells; 2019;8.
- 47. Liang J, Liu Q, Xia L, Lin J, Oyang L, Tan S, et al. Rac1 promotes the reprogramming of glucose metabolism and the growth of colon cancer cells through upregulating SOX9. Cancer Sci. Cancer Sci; 2023;114:822–36. [PubMed: 36369902]
- 48. Ren YX, Li X Bin, Liu W, Yang XG, Liu X, Luo Y. The Mechanism of Rac1 in Regulating HCC Cell Glycolysis Which Provides Underlying Therapeutic Target for HCC Therapy. J Oncol. J Oncol; 2022;2022.
- 49. Zeng RJ, Zheng CW, Gu JE, Zhang HX, Xie L, Xu LY, et al. RAC1 inhibition reverses cisplatin resistance in esophageal squamous cell carcinoma and induces downregulation of glycolytic enzymes. Mol Oncol. Mol Oncol; 2019;13:2010–30. [PubMed: 31314174]
- 50. Huang WK, Chen Y, Su H, Chen TY, Gao J, Liu Y, et al. ARHGAP25 Inhibits Pancreatic Adenocarcinoma Growth by Suppressing Glycolysis via AKT/mTOR Pathway. Int J Biol Sci. Int J Biol Sci; 2021;17:1808–20. [PubMed: 33994864]
- 51. El Hassouni B, Granchi C, Vallés-Martí A, Supadmanaba IGP, Bononi G, Tuccinardi T, et al. The dichotomous role of the glycolytic metabolism pathway in cancer metastasis: Interplay with the complex tumor microenvironment and novel therapeutic strategies. Semin Cancer Biol. Semin Cancer Biol; 2020;60:238–48. [PubMed: 31445217]
- 52. Mitaishvili E, Feinsod H, David Z, Shpigel J, Fernandez C, Sauane M, et al. The Molecular Mechanisms behind Advanced Breast Cancer Metabolism: Warburg Effect, OXPHOS, and Calcium. Front Biosci (Landmark Ed. Front Biosci (Landmark Ed); 2024;29:99. [PubMed: 38538285]
- 53. Yamamoto Y, Kawano I, Iwase H. Nab-paclitaxel for the treatment of breast cancer: efficacy, safety, and approval. Onco Targets Ther. Onco Targets Ther; 2011;4:123–36. [PubMed: 21792318]

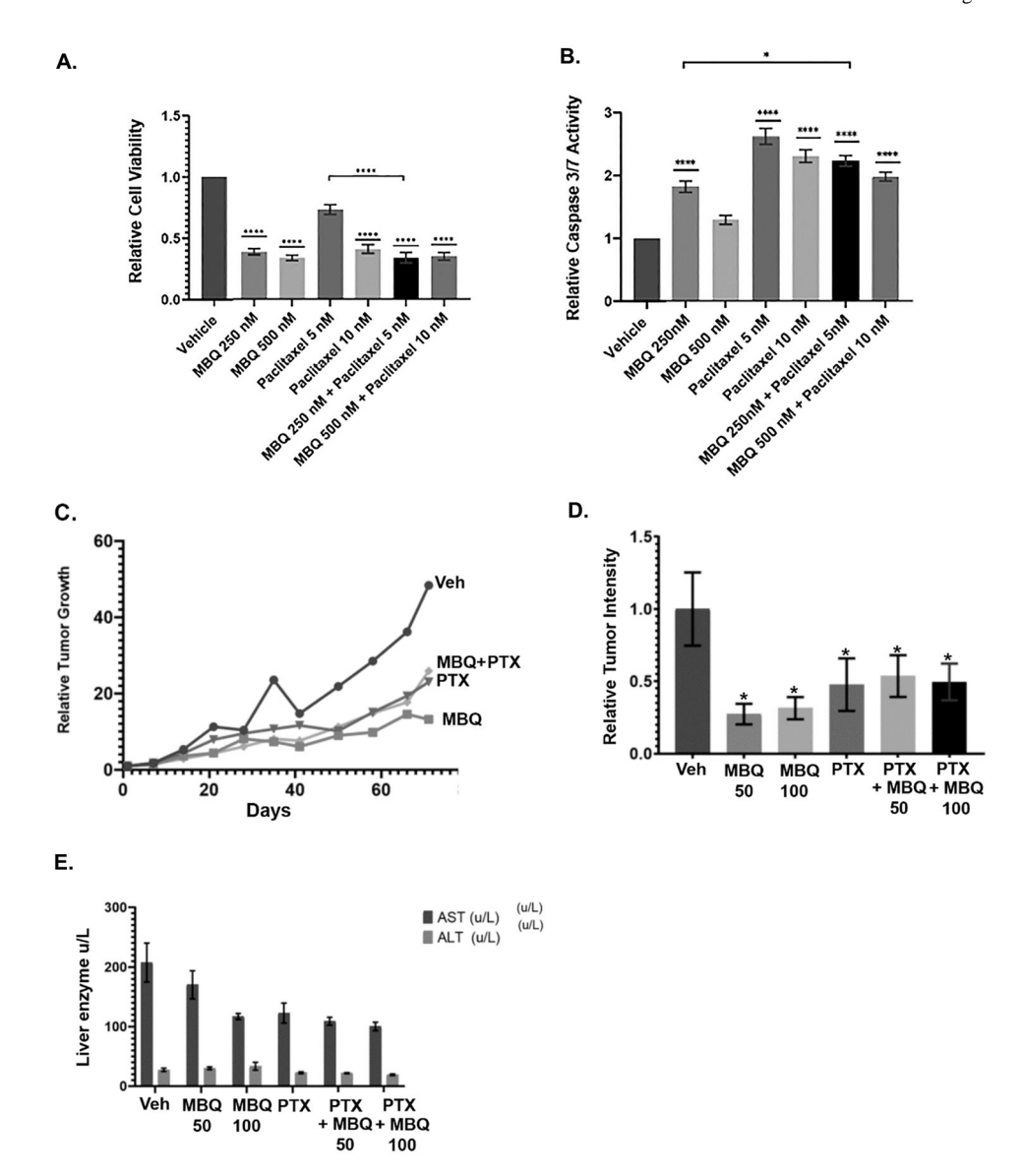


Figure 1.MBQ-167 affects MDA-MB-231 TNBC cell viability, apoptosis, and tumor growth in combination with Paclitaxel. **A, B,** MDA-MB-231 cells treated with vehicle, 250 nM MBQ-167, 5 nM Paclitaxel, or the combination (250 nM MBQ-167 + 5 nM Paclitaxel), or, 500 nM MBQ-167, 10 nM Paclitaxel, or the combination (500 nMMBQ-167 + 10 nM Paclitaxel) for 96 hrs. **A,** Cell viability as determined using MTT assay. **B,** Caspase 3/7 assays for apoptosis. N=4 ± SEM in one-way ANOVA. ****=P<0.001. **C, D, E,** Effect of MBQ-167 and Paclitaxel treatments on MDA-MB-231 mammary fat pad tumor growth. SCID mice were inoculated with GFP-MDA-MB-231 cells at the mammary fat pad, when the tumors reached ~100 mm³ in diameter, mice were randomized (N=10), and treated with vehicle, 50 or 100 mg/kg BW 5X MBQ-167 5X/week per oral, 10 mg/kg BW paclitaxel (PTX) 1X week, or the combination by I.P. **C,** Relative tumor growth as a function of days. **D,** Relative tumor size at study termination. **E,** Plasma quantification of liver enzymes Asparagine transaminase (AST) and alanine transaminase (ALT).

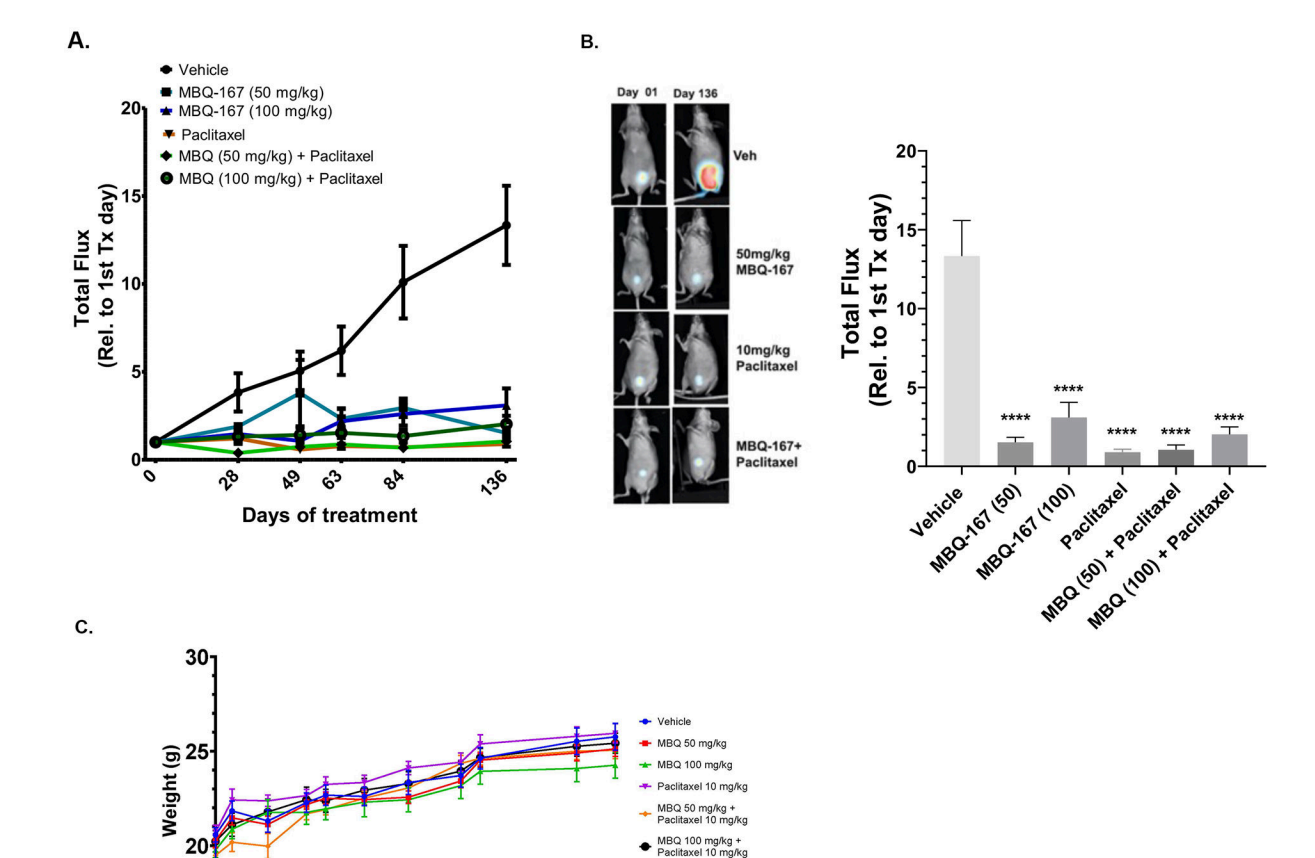
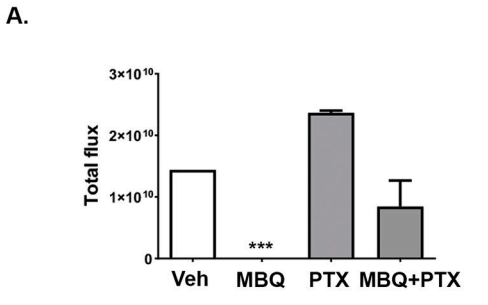


Figure 2.

Effect of MBQ-167 and Paclitaxel treatments on MDA-MB-468 mammary fat pad tumor growth. SCID mice were inoculated with luciferase tagged MDA-MB-468 cells at the mammary fat pad, when the tumors reached ~100 mm³ in diameter, mice were randomized (N=10), and treated with vehicle, MBQ-167 at 50 or 100 mg/kg BW 5X week, Paclitaxel 10 mg/kg BW 1X week for 3 weeks, with 1 week rest in each cycle, or the combination. Mice were imaged 1X a week following administration of 1.5 mg luciferin. A, Tumor growth, as measured by total flux from chemiluminescence as a function of days. B, Representative whole-body images of mice under chemiluminescence on last day (day 136) and quantification of total chemiluminescence flux on day 136 relative to day 01 for each treatment; vehicle, MBQ-167 50 mg/kg (5X a week), MBQ-167 100 mg/kg (5X a week), Paclitaxel 10mg/kg (1X a week) ****=p<0.0001. C, Mouse weights (g)/week starting from day of tumor cell inoculation.

6,6,6,6,6,6,6,6,6,6,6,6,6



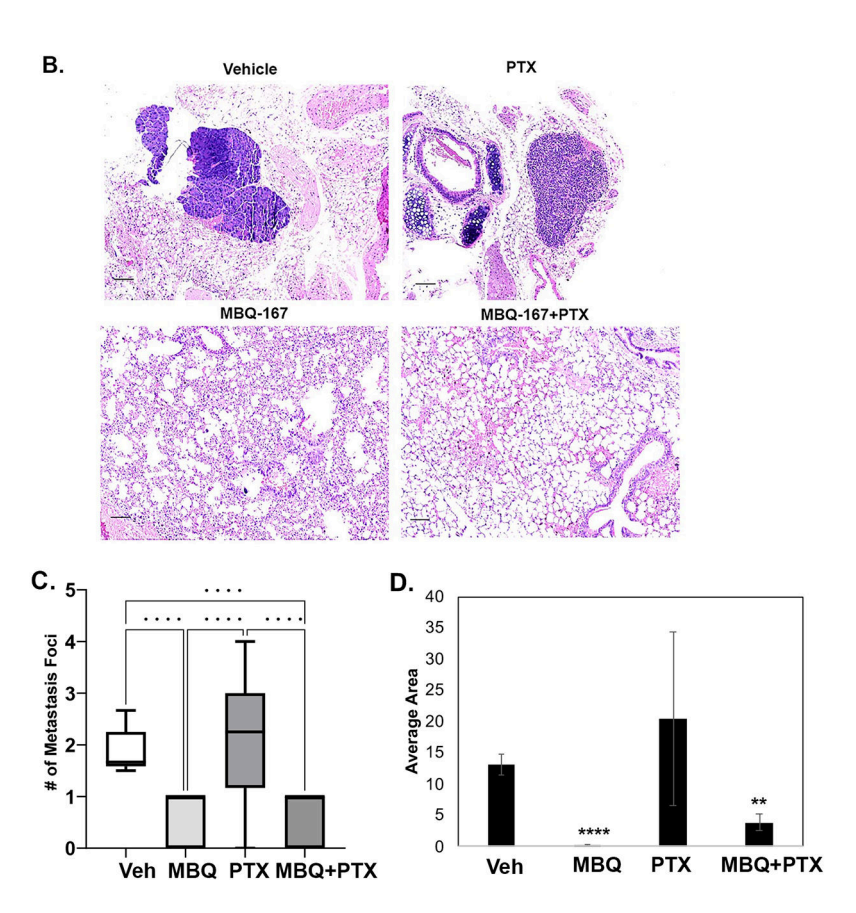


Figure 3. Effect of MBQ-167, paclitaxel (PTX), or combination on lung metastases of mice bearing luciferase-tagged MDA-MB-468 mammary fat pad tumors. **A,** Total flux from luciferase tagged lung metastases. **B,** Representative H&E sections of lungs following 136 days of vehicle, MBQ-167 50 mg/kg 5X a week, Paclitaxel 10 mg/kg 1X a week or the combination. Arrows indicate metastatic foci of 10X images acquired from a Keyence microscope system. Scale bar, 10 μ M. **C,** Number of metastatic foci/treatment; **D,** average area of lung metastases, as quantified from H&E stained lungs.

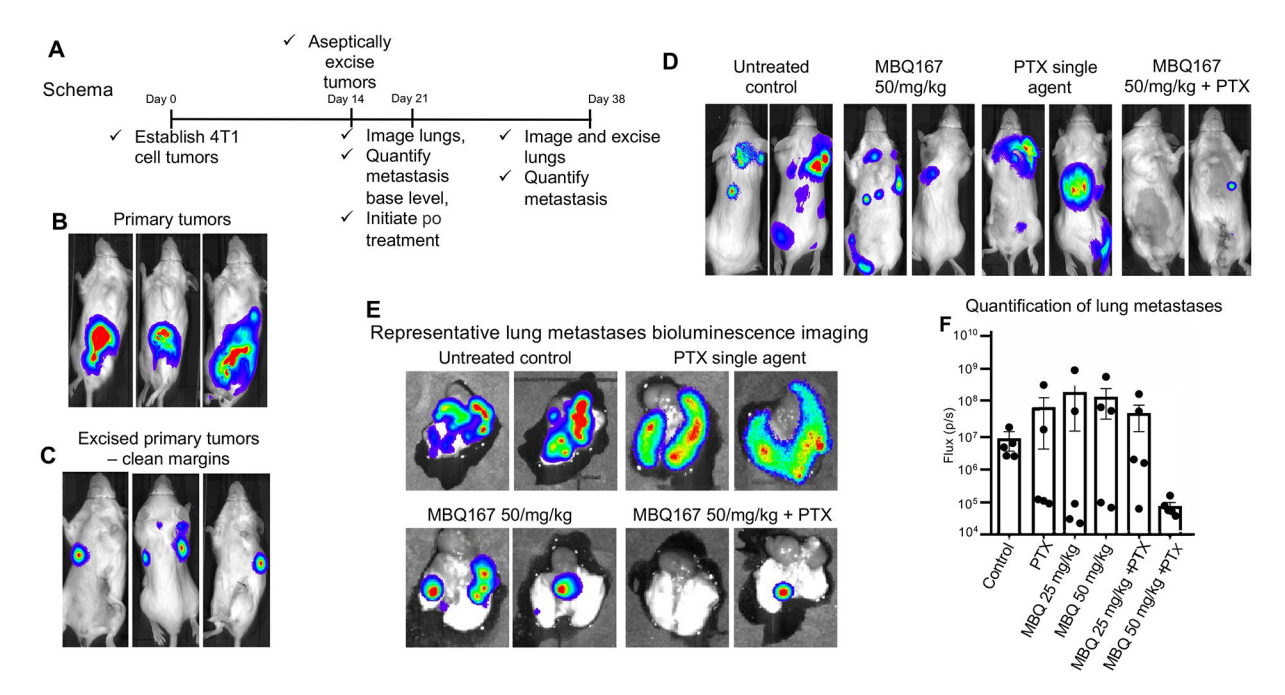


Figure 4.MBQ-167 treatment with Paclitaxel abolishes established breast cancer metastasis. **A-C**, BALB/c mice were injected in the 4th mammary fat pad with syngeneic 4T1 mammary carcinoma cells expressing firefly luciferase (150,000 cells). When the tumors reached ~150 mm³ (14d), tumors were surgically excised with tumor free margins, sutured and mice allowed to recover for 7 days. Mice were treated with 0, 25 or 50 mg/kg BW MBQ-167 5X/ week or (and) 5 mg/kg Paclitaxel 1X a week (Scheme 03 in Materials & Methods). **D**, Lung metastases were imaged on day 21 and day 38. **E**, Representative excised lungs following bioluminescence imaging. **F**, Bioluminescence profile of Flux/ps of lung metastases. N=5.

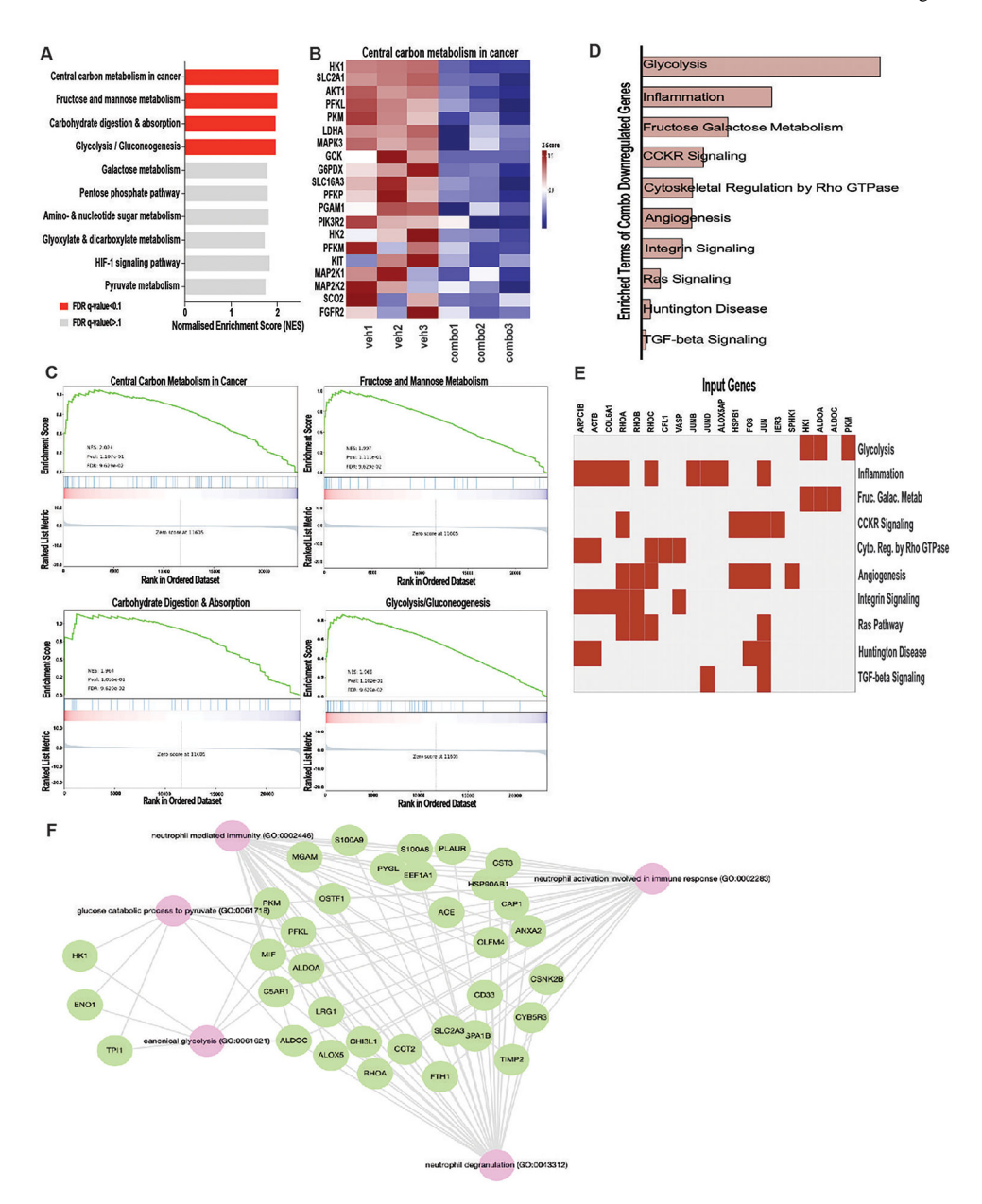


Figure 5.

RNA-Seq analysis of vehicle or combination treatment of MBQ-167 (100mg/kg) and paclitaxel (5mg/kg) in a syngeneic mouse model (4T1 cells orthotopically injected in BALB/c mice). RNA-Seq was performed on d28 tumors (N=3 from each group) that were treated for 2 weeks (Suppl. Figure 2). **A**, Results of GSEA Hallmark analysis showing enriched gene sets. Bars in red indicate significant enrichment at FDR < 10%, bars in gray represent gene sets with FDR>10%. A positive Normalized Enrichment Score (NES) value indicates enrichment in the vehicle phenotype. **B**, Heat map of the top 20 genes of the most significant regulated pathway discovered with GSEA in the comparison of vehicle (left column) vs. combo treatment (right column). Expression values are represented as colors and range from red (high expression), pink (moderate), light blue (low) to dark blue (lowest expression). **C**, Enrichment plots for significant data sets enriched in GSEA Hallmark

analysis, showing the profile of the running ES Score and positions of gene set members on the rank-ordered list. **D**, Overrepresentation (Enrichr) analysis for downregulated genes using Panther 2016. **E**, Top 20 differentially expressed genes of significantly enriched terms in the combination treatment phenotype, ordered by p-value. **F**, Enrichment map of the overrepresentation analysis using GO_Biological_Process f in EnrichR-KG.

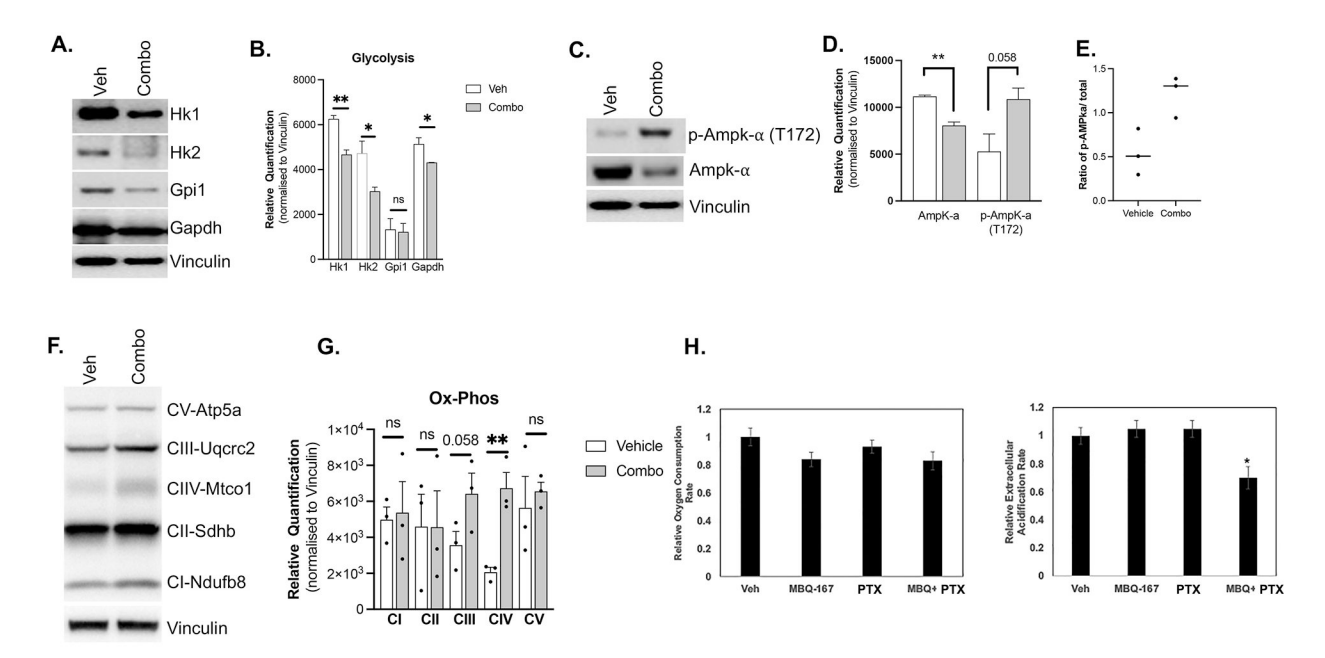


Figure 6.

A, Representative immunoblots of genes differentially expressed in 4T1 tumors in Balb/c mice treated with vehicle or combined paclitaxel and MBQ-167 (combo) (as in Suppl. Fig. 2). **B,** Quantification of protein levels, normalized to loading control (Vinculin, n=3). **C,** Western blot of AMPKα activity (phospho) and expression (total) in vehicle versus combination treatment tumors. **D,** Quantification of protein levels, normalized to loading control (Vinculin, n=3). **E,** Relative ratio of p-AMPKα in combination versus vehicle treated tumors. **F,** Western blot analysis of the relative levels of the 5 OXPHOS complexes probed for a subunit that is labile when its complex is not assembled. **G,** Quantification of protein levels, normalized to loading control (Vinculin, n=3). **H,** Seahorse analysis of MDA-MB-468 cells treated with vehicle, MBQ-167 500 nM, paclitaxel 10 nM, or the combination for 24 hrs. Left, oxygen consumption rate (OCR); right, extracellular acidification rate (ECAR) relative to vehicle (1) as measured by an Agilent Seahorse XF analyzer.